



Effect of the use in circulating fluidized bed on the performance of a VPO catalyst: Characterization and transient studies

L. Pérez-Moreno^a, S. Irusta^b, J. Soler^b, J. Herguido^a, M. Menéndez^{a,*}

^a Institute for Engineering Research of Aragón (I3A), University of Zaragoza, Spain

^b Institute of Nanoscience of Aragón (INA), University of Zaragoza, Spain

ARTICLE INFO

Article history:

Received 7 May 2008

Received in revised form

20 November 2008

Accepted 21 November 2008

Keywords:

Vanadium phosphorous oxide catalyst

Maleic anhydride

n-Butane selective oxidation

Lattice oxygen

Catalytic partial oxidation

Transient studies

ABSTRACT

The stability of the catalyst is a key issue in the operation of a circulating fluidized bed reactor (CFB) for obtaining maleic anhydride. To study the catalyst degradation process, two VPO samples have been compared: one before operation (“fresh”) and the other (“used”) after operation in a CFB. Since the operation in the CFB implies the catalyst reduction in one of the reactors and its oxidation in the other, transient experiments have been chosen as a suitable method for comparing the performance of both catalysts. In order to assess the possible modifications of properties, characterization was performed by various techniques (XPS, XRD, SEM, BET, ICP and TPR). The results show a decrease in performance of the used catalyst, with lower activity and yield and a slower oxygen transfer rate, which probably are related with morphological and structural changes such as the lower surface area, the larger size of the crystals, and the appearance of a new phase. In addition, the deposition of iron during the operation could also affect the catalyst performance.

© 2008 Elsevier B.V. All rights reserved.

1. Introduction

The partial oxidation of n-butane to maleic anhydride (MA) using VPO-based catalysts has been intensively studied for the last three decades [1–6]. At industrial level, several kinds of reactors have been utilized for MA production. Fixed beds [7] require highly diluted conditions (less than 2% butane in air) because of the risk of explosion or autoignition. Higher butane concentrations can be used with fluidized bed reactors (up to 4% butane in air) due to a better heat removal and ease of reaction temperature control [8]. In these reactors, two reactions (catalyst reduction and catalyst oxidation) occur simultaneously. The n-butane oxidation and catalyst oxidation rates must be equal at steady state, but the rate of the process (as a whole) is frequently controlled by just one of these steps. This fact results in large excesses of oxygen being used to maintain reasonable reaction rates and to maintain the catalyst near its optimum oxidation state [9]. This strategy, that is employed in conventional reactors (fixed or fluidized bed), implies a large dilution of butane, and therefore the need to manage large volumes in the reactor effluent.

A possible remedy to reduce the dilution of butane is to use the catalyst lattice oxygen. Using this idea, DuPont developed a full scale commercial plant to produce MA in a circulating fluidized bed

(CFB) reactor. This system consists of a riser reactor in which the catalyst under controlled oxygen concentration oxidizes butane to MA, using mainly the oxygen from the catalyst lattice, and a fluidized bed in which the catalyst is re-oxidized [10]. This process demands a detailed knowledge of both the transient reduction and oxidation kinetics for butane oxidation to MA on VPO catalysts. However, the studies carried out under steady state reaction conditions may not be applicable to the sequentially operated process [11]. This is because the gas phase composition affects significantly the VPO catalyst surface structure, thus the catalyst may behave differently under transient conditions than under steady state operating conditions [12]. Another reactor type that may operate outside the flammability limits is the membrane reactor [13–15], but this type of contactor has not yet been developed for large-scale operations. Finally, a new concept of fluidized reactor has been proposed for this reaction, the two zone fluid bed reactor (TZFBR). This consists of separating the reaction and regeneration zones within the same vessel, taking advantage of the fact that oxygen can be transferred in the lattice of the catalyst by using the internal solid circulation characteristic of fluidized beds [16].

There has been some controversy about the active phase and the reaction mechanisms. The activity in the reaction of MA production is commonly attributed to well crystallized $(VO)_2P_2O_7$, which is a V^{4+} phase, but three oxidation states (V^{3+} , V^{4+} and V^{5+}) have been identified under reaction conditions [17]. In fact, the role of each oxidation state has been the subject of controversy. Some authors have suggested that a V^{4+} phase is catalytically active and that the

* Corresponding author. Tel.: +34 976761152; fax: +34 976762142.
E-mail address: qtmiguel@unizar.es (M. Menéndez).

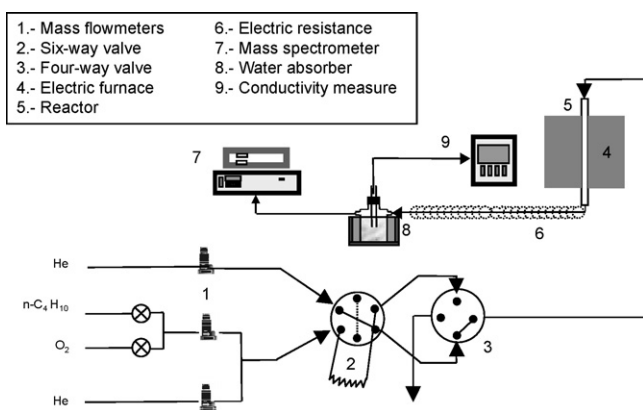


Fig. 1. Scheme of the pulse experimental set-up.

presence of V^{5+} phases are detrimental to the catalytic performance [18]. In contrast, other authors believe that V^{5+} plays a beneficial role in the performance and that the V^{4+} presence is negative [19]. It has recently been proved that the active centre for butane activation and maleic anhydride formation comprises a V^{4+}/V^{5+} couple that is well dispersed on the surface of a range of VPO phases, which for well-equilibrated catalysts is $(VO)_2P_2O_7$ [20].

Apart from this controversy, there is a strong interest in to test if the VPO catalyst loses activity and/or selectivity after being used in anaerobic operations for MA production. The goal of the present study is to investigate the changes in oxidation capacity, morphology and structure that VPO catalyst suffers after several months in operation with reaction–regeneration cycles by comparing this used catalyst with the unused (fresh) catalyst.

2. Experimental

The two samples of VPO catalyst, one fresh and the other used during several months in an industrial CFB, were provided by the Chemical Engineering Department of the École Polytechnique of Montreal (Canada). They were $(VO)_2P_2O_7$ with a shell of amorphous silica (c.a. 5 wt%). The characterization was made by the different techniques described below.

Unsteady state tests were carried out in order to calculate the oxidation and reduction capacity by means of pulses of both oxygen and n-butane at different temperatures. For each pulse, the instantaneous conversion and selectivity for the main products was obtained. The scheme of the experimental set-up used is shown in Fig. 1. The sample (generally 1 g) was located in an 8 mm i.d. reactor made of quartz, which was placed in an electric furnace. The carrier (He) flowrate was 200 mL(STP)/min. The reaction temperature used was 350–450 °C and atmosphere pressure. Gases were injected by means of several mass flow controllers. A six-way valve was used to release periodically a known quantity of reacting gas mixture (helium + n-butane or helium + oxygen) by means of a “loop” of 1 mL in volume, whereas in the remaining time the sample was kept under a continuous inert carrier gas current (helium). Another four-way valve was used to provide an exchange between the carrier helium and the reacting gas mixture streams when required. After the reactor, the outlet gases were kept hot by an electrical resistance in order to avoid the condensation of products. A small quantity of gas was taken for analysis in mass spectroscopy equipment (Thermo Onix model VG Gas ProLab). The rest of the gas stream was passed through an absorber containing distilled water where the condensable products (mainly MA) were retained. The concentration of MA in this water was measured with a Crison conductivity meter model GLP 31, after calibrating the conductivity probe. HPLC analysis showed only negligible amounts of other adsorbed products.

Table 1
Oxygen consumption in the reoxidation step.

T (°C)	mmol O ₂ /kg VPO catalyst	
	Fresh catalyst	Used catalyst
350	14.3	3.6
400	32.9	9.0
450	35.6	7.4

X-ray photoelectron analysis (XPS) was performed with an Axis Ultra DLD (Kratos Tech.) working with a monochromatic AlK α radiation (10 kV, 15 mA) and the charge compensation device provided by the supplier. The samples were mounted on a sample rod placed in the pretreatment chamber of the spectrometer and then evacuated at room temperature. The pressure in the analysis chamber was around 10^{-6} Pa. The angle between the normal to the sample surface and the lens axis was 0°. For the individual peak regions, a pass energy of 20 eV was used. The survey spectrum was measured at 160 eV pass energy. Analyses of the peaks were performed with the software provided by the manufacturer, using a weighted sum of Lorentzian and Gaussian component curves after background subtraction. The binding energies (BE) were referenced to the internal C 1s (284.5 eV) standard.

Scanning electron microscopy (SEM, Hitachi S-2300) was performed to analyze the surface roughness and grain size. Moreover, X-ray diffraction analysis (Rigaku/Max System diffractometer Cu K α radiation $\lambda = 1.5418$ Å and graphite monochromator), was carried out (not shown here) to check the crystallinity and purity of the powders as provided. The specific surface areas of the powders were obtained by static N₂ adsorption measurements with a Micromeritics ASAP 2020 on samples previously evacuated at 250 °C for 8 h. Atomic composition of the samples was determined by inductively coupled plasma (ICP) analysis using PerkinElmer Elan 6000 equipment.

Thermal programmed reduction (TPR) was carried out in a specific facility composed of a quartz reactor placed in an electric furnace, a temperature control unit (RCK Instrument Inc., Model REX-P9), mass flow controllers to inject both argon and hydrogen, and a thermal conductivity detector (GOW MAC Instrument Co., Model 10-454-2). The data were acquired every second by specific software made in Lab-Windows.

3. Results and discussion

A comparison of catalysts employed in a CFB, where the solid is subjected to oxidation–reduction cycles, must be done in a system where the catalyst varies its oxidation degree with time, where the consumption of lattice oxygen can be calculated and the changes in both activity and selectivity in absence of gas phase oxygen can be related with the oxidation degree. This can not be done in a typical fixed bed with cofeeding of butane and air in steady state. We have employed a system able to send pulses of reactive gas (butane or

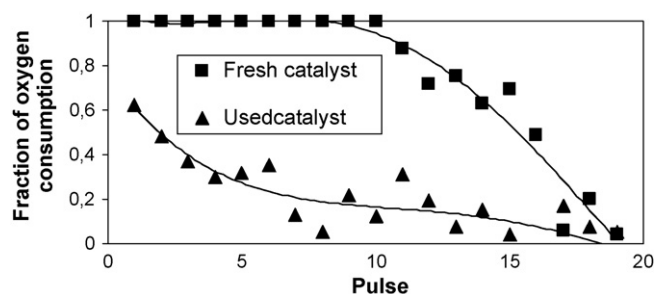


Fig. 2. Evolution of the oxygen consumption in reoxidation step at 400 °C.

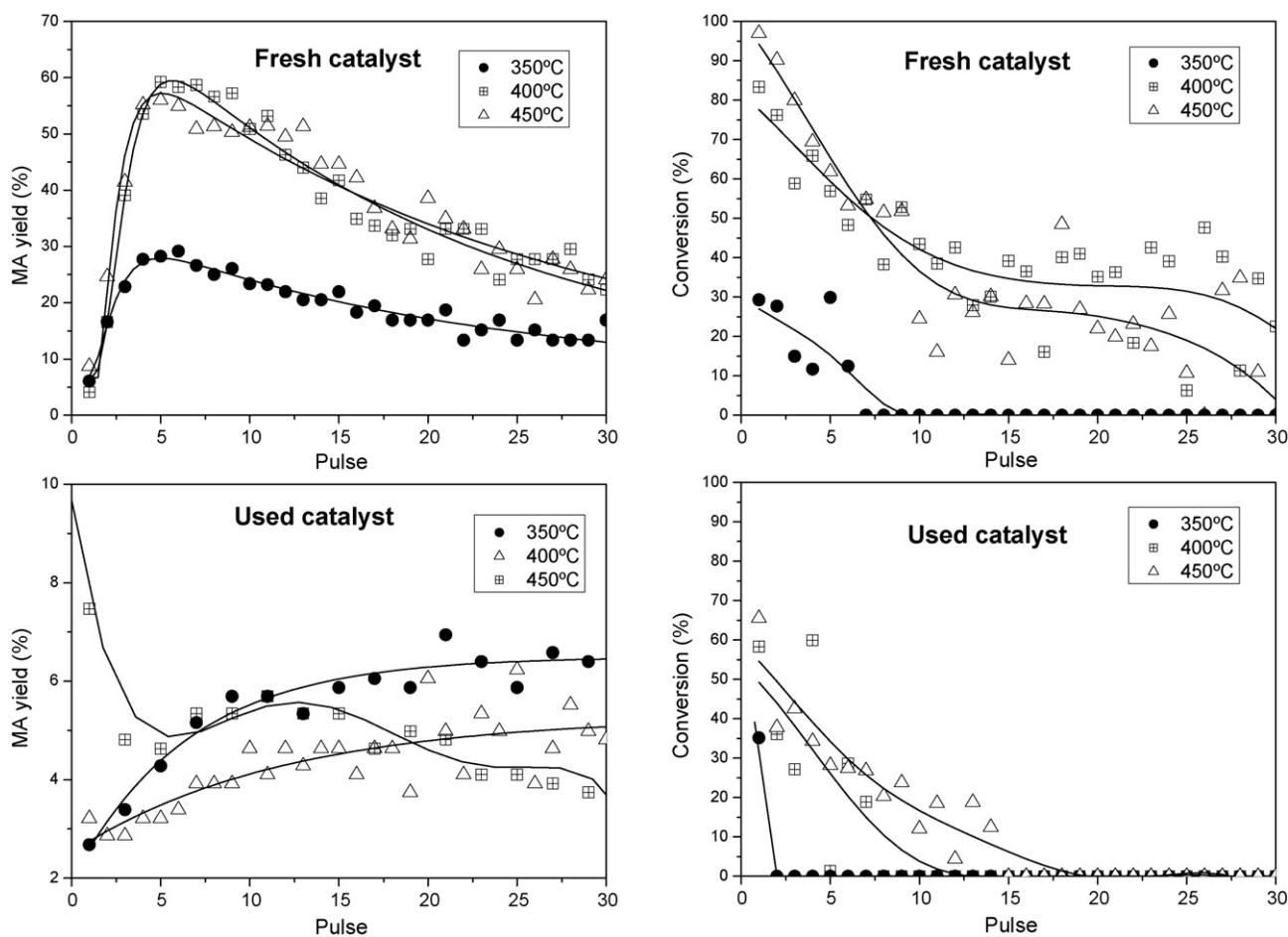


Fig. 3. Evolution of the MA yield and conversion in reaction step (lines are only for visual help).

oxygen) in order to calculate the oxygen consumption of both VPO samples, as received, the instantaneous n-butane conversion and product selectivity at various degrees of catalyst reduction and the oxygen consumption in reoxidation. Experiments were designed with three steps: (1) *oxidation step* of the sample with 20 pulses of oxygen (5% in helium) in order to calculate the oxygen capture at three temperatures: 350 °C, 400 °C and 450 °C followed by a continuous oxygen flow (5%) to achieve complete VPO oxidation and, finally, 5 pulses of oxygen (5%) in order to calculate the response factor of the mass spectrometer and thus quantify the oxygen capture in the previous 20 pulses; (2) *reaction step*, injecting 30 n-butane pulses (5% in helium) at the same temperatures as in the previous step, to study the instantaneous conversion and the yield to MA in anaerobic atmosphere; (3) *reoxidation step*, the same as in the first step, but measuring also the mass 44 corresponding to the CO₂ that could be formed by the coke combustion. For every experiment, the area of the pulses was calculated by integration and compared with the pulses without consumption. The total amount formed or consumed of each compound results from the sum of the values for all the pulses.

Table 2
MA yield (%) in the reaction step.

T (°C)	Fresh catalyst	Used catalyst
350	19.1	5.6
400	37.6	4.3
450	36.3	5.0

The results obtained for the first oxidation step showed a negligible oxygen consumption for both catalysts, which indicates that both were in a high oxidation state. However, after the reaction step with n-butane in anaerobic conditions, their oxidation state was lower, as can be seen by the oxygen consumption data presented in Table 1. It can be observed that, for both catalysts tested, the oxygen consumption was significantly smaller below 400 °C. This is in accordance with a slower oxidation rate at these temperatures described in previous works [11]. The comparison between both catalysts shows a sharp loss of oxygen consumption for the used catalyst, which can have a significant influence on the redox performance of the catalyst during the reactor operation. The evolution of the oxygen consumption at 400 °C is shown in Fig. 2. A total consumption of oxygen can be observed with fresh catalyst in the first 10 pulses, whereas the consumption is gradually reduced for the following ones. In contrast, the fraction of oxygen consumed in each pulse with the used catalyst is initially markedly smaller, which indicates a slower oxidation rate, and approaches a very small value much sooner. This means that the diffusion of oxygen to the surface is faster in the fresh catalyst than in the used one. In all cases, the amount of oxygen is quite small compared with the stoichiometric amount needed to change the oxidation state of all the vanadium. The maximum amount of oxygen transferred (35.6 mmol/kg) is roughly 1% of the oxygen needed to change the oxidation state of vanadium from V⁴⁺ to V⁵⁺, which implies that only a few atomic layers close to the surface are involved in the reaction.

For the reaction step, the evolution of the MA yield and n-butane conversion are shown in Fig. 3. Due to experimental difficulties

Table 3
XPS analysis of the tested catalysts.

Catalyst	Binding energy, FWHM (eV) ^a			V_{ox} ^b	Surface ratio			
	O 1s	P 2p	V 2p _{3/2}		O/V	P/V	Si/V	
Fresh	531.2 (2.6)	134.0 (1.8)	516.8 (1.4)	518.0 (1.3)	4.36	8.47	1.37	0.85
Used	531.3 (2.8)	134.0 (1.9)	516.8 (1.5)	517.9 (1.6)	4.54	8.71	1.40	0.84
Fresh (after reaction step)	531.4 (2.7)	133.9 (1.9)	516.7 (1.6)	517.8 (1.5)	4.30	7.76	1.46	0.45
Used (after reaction step)	531.1 (1.9)	133.8 (1.8)	516.7 (1.6)	517.9 (1.4)	4.26	7.96	1.53	0.48

^a Referenced to BE of C 1s 284.5 eV, numbers between brackets are the full widths at half maximum.

^b Effective oxidation state of vanadium calculated from the percentage of the total area of V 2p_{3/2} peak (taken as 100%).

the conversion values have some uncertainty, but the trends are very clear. The fresh catalyst is more efficient than the used one at all the temperatures, providing much higher conversion and yield. This result indicates the loss of activity of VPO during operation in an industrial reactor. The total MA yield in 30 pulses of n-butane (5%) is shown in Table 2. It can be noticed that the quantity of MA obtained with the fresh catalyst is considerably higher than with the used one. With the used catalyst, the MA yield, always low, scarcely varies with temperature, which suggests that the oxygen diffusion (a physical process) is the controlling factor.

XPS analysis was carried out in order to identify possible changes occurring on the surface of the catalysts after being in contact with the reactant stream. The main elements detected in the fresh and used catalysts were O, P, V, Si, N and C, while Fe appeared only in

the used catalyst. The XPS results are shown in Table 3. The P 2p and O 1s BEs of all the catalysts were essentially the same in all the samples studied.

All the V 2p_{3/2} peaks (not shown) have an asymmetric shape that points to the presence of different single components. The main problem that appears in this analysis results from the multiplet splitting that leads to different line shapes of the V⁵⁺, V⁴⁺ and V³⁺ components and makes it very difficult to develop a set of fitting parameters for each valence state [21]. To overcome this problem, Coulson et al. [22] elaborated a correlation between the first moment of the O 1s and V 2p_{3/2} peaks. Unfortunately, in our case the position of the O 1s peak may be strongly influenced by the oxygen in the SiO₂ support. Therefore, in this work the analysis of the XPS spectra has been performed by a curve-fitting procedure in order to distinguish vanadium species in different oxidation states. All the spectra can be deconvoluted into two components at 516.7–516.8 and 517.9–518.0 eV which can be assigned to V⁴⁺ and V⁵⁺ species, respectively [21,23,24].

These deconvolutions show different contents of V⁴⁺ and V⁵⁺ in fresh and used catalysts both before and after the reaction step, which lead to changes in the effective oxidation state (Table 3). The fresh catalysts present a mean oxidation state of vanadium (V_{ox}) of 4.36, a slightly higher value than those previously reported for non-supported VPO catalysts [25]. However, Casaletto et al. [26] found a value of 4.4 in alumina supported catalysts prepared in an aqueous medium. In addition, Suchorski et al. [21] reported values of V_{ox} as high as 4.76 in a VPO catalyst layer (organic preparation) on a tubular membrane. The oxidation state of vanadium on the surface decreases after the reaction step for both catalysts, but the change was smaller in the fresh catalyst, in spite of the fact that it had released more oxygen. The explanation for this surprising result could be the higher oxygen diffusivity in the fresh catalysts,

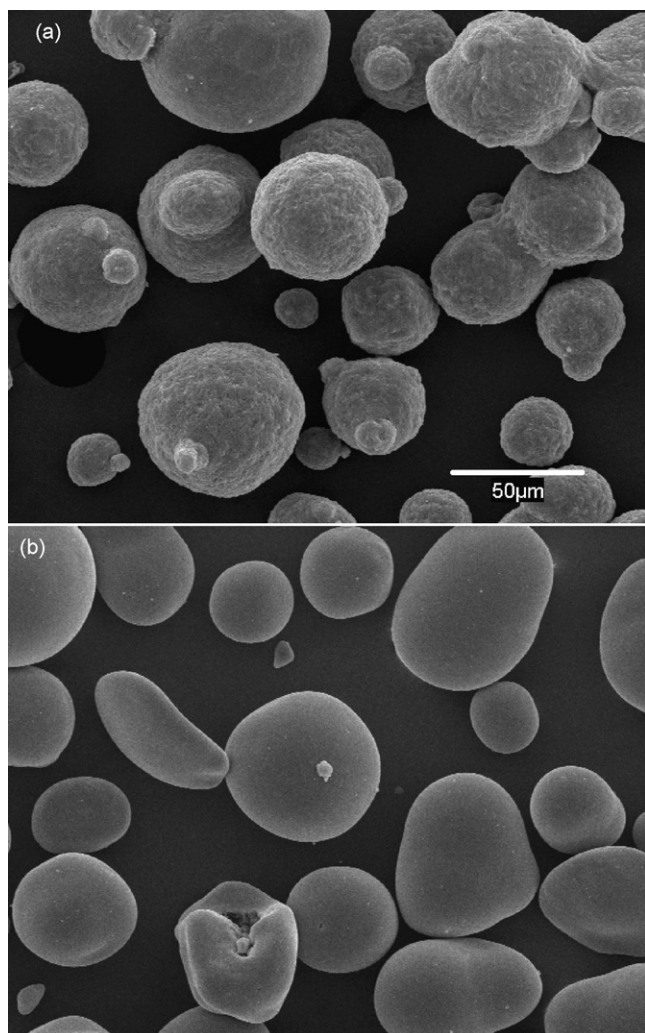


Fig. 4. SEM micrographs of both catalysts characterised: (a) fresh and (b) used.

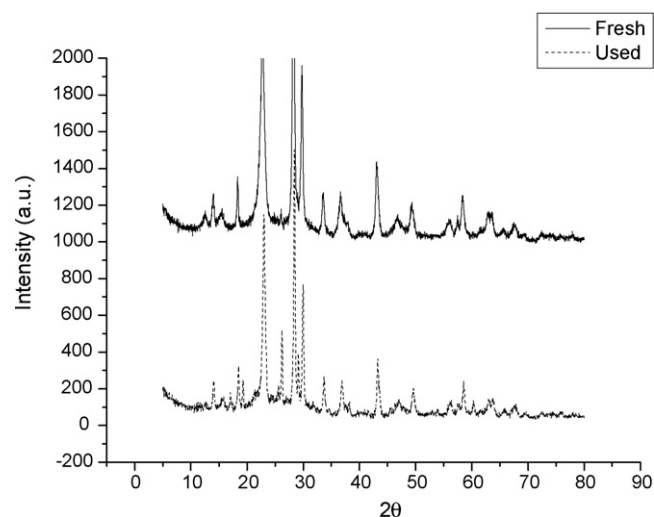


Fig. 5. XRD patterns.

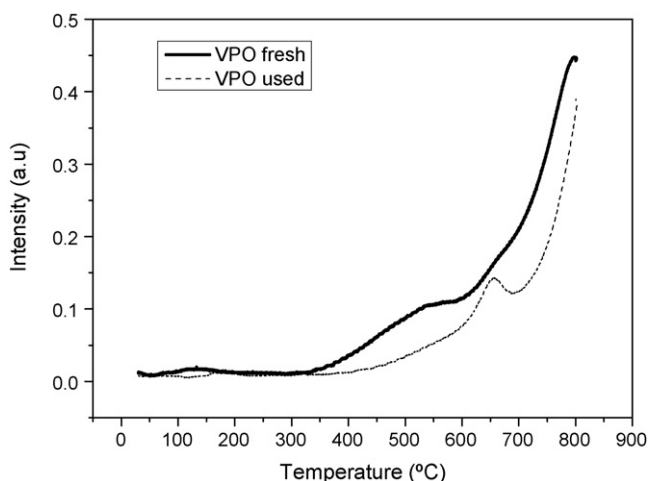


Fig. 6. TPR study.

which in turn could be due to the smaller size of the crystallites, as will be shown below.

The reduction treatment not only diminished slightly the vanadium oxidation state and the O/V ratio, but also increased the superficial phosphorous concentration and strongly reduced the Si/V external ratio. It is known that the excess P not only prevents the oxidation of the bulk but also limits the total oxidation of the surface under severe conditions [27]. On the other hand, the migration of vanadium phases to the surface of the catalyst (lower Si/V ratio) would increase the activity of catalysts.

The Fe detected on the used catalysts, most likely as iron oxide (BE = 711.7 eV), is in low superficial atomic concentration, less than 1.2%. The presence of iron was also detected by the ICP technique (0.08% Fe in fresh catalyst, 0.7 wt%). Iron can be used as dopant to increase the maleic anhydride yield [28], but in this case the much larger concentration of iron in the used sample suggests that it has been deposited during the operation (perhaps from the CFB reactor walls). Since iron oxides have catalytic activity in the deep oxidation of alkanes [29], it could be one of the causes of the decrease in the MA yield in the used catalysts.

The different performance of both catalysts studied could also be explained by morphological changes. In this context, two SEM photographs are presented in Fig. 4. It can be clearly seen that the particle surface of the used sample shows less roughness. This could be due to two possible effects: recrystallization of the catalyst during the oxidation/reduction cycles, and/or the friction of particles in the CBF (as commented above), however it may only be a change located in the surface of the spherical particles, and not related with the characteristics of the internal surface. A more significant change is the decrease in specific surface. The BET area changes very significantly, giving values of 24.8 and 4.3 m²/g for fresh and used catalysts, respectively. This fact can explain the strong decrease in catalyst activity, and suggests that the repeated cycles of reduction and oxidation resulted in an increased size of the crystallites.

As an additional measurement, the crystallinity of both samples was determined by XRD (Fig. 5). Using the Scherrer equation for the more intense peak ($2\theta = 28^\circ$), it was estimated that the mean diameter grew from 325 to 495 Å after operation in the CFB. This increase in the size of the crystals has, as a consequence, the removal of catalyst active sites which causes the drop in activity. The slower rate of oxygen transfer can also be related with the smaller surface/volume ratio, since oxygen diffusion should occur from deeper layers. A second change that can be observed in the XRD is the appearance of peaks corresponding to a new phase, VOPO₄. Since it is generally accepted that the most active phase is (VO)₂P₂O₇, such structural change should also affect the performance.

The reduction of the catalyst in a temperature programmed experiment (TPR) has also been used to compare the reducibility of both catalysts. As can be seen by the TPR analysis (Fig. 6), the H₂ consumption occurs at higher temperatures in the used catalyst, in accordance with the other experiments previously presented.

4. Conclusion

Transient experiments for the two VPO catalyst samples, “fresh” and “used”, have shown a dramatic decrease in maleic anhydride yield and oxygen transfer capacity for the used sample at all the temperatures studied. In order to determine the causes of this fact, several characterization studies have been carried out by different techniques. XPS and ICP verify the presence of iron in the used catalyst (Fe/V = 0.2 in surface and 0.7 wt% for the bulk). The presence of iron oxide, known to be catalyst for the total oxidation of organic compounds, can be one of the reasons for the decrease in MA selectivity. A strong decrease in BET area (24.8–4.3 m²/g) after the CFB operation and the growth of crystallites, calculated from XRD patterns, explain the decrease in the reaction rate and the slower transport of oxygen to replenish the surface. XRD also show the presence of a new VOPO₄ phase in the used catalyst. The worsening of the redox performance is also corroborated by slower hydrogen consumption in a TPR study. All the above changes confirm that the VPO catalyst has been affected by the operation in the CFB reactor and suffered morphological and structural changes that provoke a decrease in the number of active sites and a worse redox performance.

Acknowledgements

Jaime Soler thanks the Ramón y Cajal Program for the support received. This work has been partially funded by the Spanish Ministry of Education and Science (project CTQ 2004-01721).

References

- [1] F. Cavani, G. Centi, F. Trifirò, *Appl. Catal. A* 9 (1984) 191–202.
- [2] B.K. Hodnett, *Catal. Today* 1 (5) (1987) 527–536.
- [3] G. Centi, F. Trifirò, J.R. Ebner, V.M. Franchetti, *Chem. Rev.* 88 (1988) 55–80.
- [4] G.J. Hutchings, *Appl. Catal. A* 72 (1991) 1–32.
- [5] G. Centi, *Catal. Today* 16 (1) (1993) 5–26.
- [6] F. Trifirò, *Catal. Today* 41 (1998) 21–35.
- [7] J.C. Burnett, R.A. Keppel, W.D. Robinson, *Catal. Today* 1 (5) (1987) 537–586.
- [8] R.M. Contractor, A.W. Sleight, *Catal. Today* 1 (5) (1987) 587–607.
- [9] R.M. Contractor, H.S. Horowitz, G.M. Sisler, E. Bordes, *Catal. Today* 37 (1) (1997) 51–57.
- [10] R.M. Contractor, D.I. Garnett, H.S. Horowitz, H.E. Bergna, G.S. Patience, J.T. Schwartz, G.M. Sisler, in: V. Cortés Corberan, S. Vic Bellón (Eds.), *New Developments in Selective Oxidation II*, Elsevier, Amsterdam, 1994, pp. 233–242.
- [11] D. Wang, M.A. Barteau, *Appl. Catal. A* 223 (1–2) (2002) 205–214.
- [12] D. Wang, M.A. Barteau, *J. Catal.* 197 (2001) 17–25.
- [13] R. Mallada, M. Menéndez, J. Santamaría, *Catal. Today* 56 (2000) 191–197.
- [14] A. Cruz-López, N. Guilhaume, S. Miachon, J.-A. Dalmon, *Catal. Today* 107–108 (2005) 949–956.
- [15] M. Alonso, M.J. Lorences, G.S. Patience, A.B. Vega, F.V. Díez, S. Dahl, *Catal. Today* 104 (2005) 177–184.
- [16] J. Gascón, C. Téllez, J. Herguido, M. Menéndez, *Ind. Eng. Chem. Res.* 44 (2005) 8945–8951.
- [17] M.J. Lorence, G.S. Patience, F.V. Díez, J. Coca, *Appl. Catal. A: Gen.* 263 (2004) 193–202.
- [18] V.V. Gulliants, J.B. Benziger, S. Sundaresan, I.E. Wachs, J.-M. Jehng, J.E. Roberts, *Catal. Today* 28 (1996) 275–295.
- [19] G.W. Coulston, S.R. Bare, H. Kung, K. Birkeland, G.K. Bethke, R. Harlow, N. Herron, P.L. Lee, *Science* 275 (1997) 191–193.
- [20] G.J. Hutchings, C.J. Kiely, M.T. Sananes-Schulz, A. Burrows, J.C. Volta, *Catal. Today* 40 (1998) 273–337.
- [21] Y. Suchorski, B. Munder, S. Becker, L. Rihko-Struckmann, K. Sundmacher, H. Weis, *Appl. Surf. Sci.* 253 (13) (2007) 5904–5909.
- [22] G. Coulston, E. Thompson, N. Herron, *J. Catal.* 163 (1996) 122–129.
- [23] K. Ait-Lachgar-Ben Abdelouahad, M. Roulet, M. Brun, A. Burrows, C.J. Kiely, J.C. Volta, M. Abon, *Appl. Catal. A* 210 (2001) 121–136.

- [24] M. López Granados, J.L.G. Fierro, F. Cavani, A. Colombo, F. Giuntoli, F. Trifirò, *Catal. Today* 40 (1998) 251–261.
- [25] C. Carrara, S. Irusta, E. Lombardo, L. Cornaglia, *Appl. Catal. A* 217 (2001) 275–286.
- [26] M.P. Casaletto, S. Kaciulis, L. Lisi, G. Mattogno, A. Mezzi, P. Patrono, G. Ruoppolo, *Appl. Catal. A* 218 (1–2) (2001) 129–137.
- [27] L.M. Cornaglia, E.A. Lombardo, *Appl. Catal. A* 127 (1995) 125–138.
- [28] Y. Kamiya, Y. Kijima, T. Ohkura, A. Satsuma, T. Hattori, *Appl. Catal. A* 253 (1) (2003) 1–13.
- [29] A.L. Barbosa, J. Herguido, J. Santamaría, *Catal. Today* 64 (2001) 43–50.